Carbohydrate Polymers 99 (2014) 242–248

Contents lists available at ScienceDirect

Carbohydrate Polymers

journal homepage: www.elsevier.com/locate/carbpol

Shape-memory starch for resorbable biomedical devices

A. Beilvert[a], F. Chaubet[b,c], L. Chaunier[a], S. Guilois[a], G. Pavon-Djavid[b,c], D. Letourneur[b,c], A. Meddahi-Pellé[b,d], D. Lourdin[a,*]

[a] INRA, UR1268, Unité Biopolymères Interactions et Assemblages, rue de la géraudière, 44300 Nantes, France
[b] INSERM, U698, Bioengineering for Cardiovascular and Therapy Team, 46 rue H. Huchard, 75877 Paris, France
[c] Institut Galilée, Université Paris 13, Sorbonne Paris Cité, 99 avenue JB Clément, 93430 Villetaneuse, France
[d] Institut Universitaire de Technologie de Saint-Denis, Université Paris 13, Sorbonne Paris Cité, Place du 8 mai 1945, 93206 Saint-Denis, France

ARTICLE INFO

Article history:
Received 13 February 2013
Received in revised form 24 July 2013
Accepted 8 August 2013
Available online 19 August 2013

Keywords:
Biomaterial
In vivo implantation
Shape-memory
Starch
Extrusion

ABSTRACT

Shape-memory resorbable materials were obtained by extrusion-cooking of potato starch with 20% glycerol under usual conditions. They presented an efficient shape-memory with a high recovery ratio (Rr > 90%). Their recovery could be triggered at 37 °C in water. After water immersion at 37 °C, the modulus decreased from 1 GPa to 2.4 MPa and remained almost constant over 21 days. Gamma-ray sterilization did not have a dramatic impact on their mechanical properties, despite a large decrease of molecular mass analyzed by asymmetrical flow field-flow fractionation coupled with multi-angle laser light scattering (AFFFF-MALLS). Samples implanted in a rat model exhibited normal tissue integration with a low inflammatory response. Thus, as previously investigated in the case of shape-memory synthetic polymers, natural starch, without chemical grafting, can now be considered for manufacturing innovative biodegradable devices for less-invasive surgery.

1. Introduction

Starch is a natural, renewable and biodegradable polymer produced by many plants as a source of stored energy. It is the second most abundant biomass component in nature. It is found in plant roots, stalks, crop seeds, and staple crops such as rice, corn, wheat, cassava, or potato (Buléon, Colonna, Planchot, & Ball, 1998). Starch is a polyanhydroglucose that consists of two homologous polymers: the linear amylose and the hyper-branched amylopectin, whose molecular weights (Mw) range from 10^4 to 10^6 g mol^{-1} and from 10^7 to 10^9 g mol^{-1}, respectively. In its native form, starch is stored as granules and presents a semi-crystalline structure. As an inexpensive resource, it is widely utilized for the development of biodegradable materials such as soluble films (Lopez, Lecot, Zaritzky, & Garcia, 2011), as well as innovative materials for biomedical applications. To achieve these, numerous methods are used to create starch-based biomaterials, including wet spinning (Ghosh et al., 2008), fiber meshing (Oliveira et al., 2007; Santos et al., 2010), injection molding (Neves, Kouyumdzhiev, & Reis, 2005), casting (Arockianathan, Sekar, Kumaran, & Sastry, 2012; Martins et al., 2012) and extrusion (Gomes, Ribeiro, Malafaya, Reis, & Cunha, 2001; Hayakawa, Linko, & Linko, 1996). They lead to various structures ranging from partially crystalline to a completely amorphous state.

Shape-memory polymers (SMPs) represent an important group of stimuli-responsive materials. After being deformed into a temporary shape, SMP recover their initial shape, known as their permanent shape, when exposed to a specified stimulus such as temperature, pH, humidity, *etc.* (Lendlein & Kelch, 2002). The molecular structure responsible for shape-memory properties combines a permanent network and a temporary one. The hard permanent network stores the permanent initial shape in memory when the material is deformed to its temporary shape, after being heated above its transition temperature (T_{trans}). The temporary network is fixed in the temporary shape when the SMP is cooled below T_{trans} under a maintained mechanical strain. When heated again above T_{trans}, the temporary network relaxes allowing the material to spontaneously return to its permanent shape (Guo et al., 2011; Lendlein & Kelch, 2002). In thermally-induced amorphous SMP, the glass transition temperature (Tg) is closely related to T_{trans} (Leng, Lan, Liu, & Du, 2011; Vechambre, Buleon, Chaunier, Gauthier, & Lourdin, 2011). Thermally-activated SMP are of great interest in the field of biomaterials (Lendlein, Behl, Hiebl, & Wischke, 2010; Leng

Abbreviations: wb, wet basis; RH, relative humidity; DMA, dynamic mechanical analysis; SMP, shape-memory polymers; Tg, glass transition temperature; T_{Trans}, transition temperature.

* Corresponding author. Tel.: +33 02 40 67 51 47; fax: +33 02 40 67 50 05.
E-mail addresses: anne.beilvert@nantes.inra.fr (A. Beilvert), frederic.chaubet@univ-paris13.fr (F. Chaubet), laurent.chaunier@nantes.inra.fr (L. Chaunier), sophie.guilois@nantes.inra.fr (S. Guilois), graciela.pavon@univ-paris13.fr (G. Pavon-Djavid), didier.letourneur@inserm.fr (D. Letourneur), anne.pelle@inserm.fr (A. Meddahi-Pellé), denis.lourdin@nantes.inra.fr (D. Lourdin).

0144-8617/$ – see front matter © 2013 Elsevier Ltd. All rights reserved.
http://dx.doi.org/10.1016/j.carbpol.2013.08.015

et al., 2011) due to a combination of adaptable T_{trans}, large shape deformation and tunable stiffness (Liu, Qin, & Mather, 2007). For medical applications, direct activation of thermally-induced SMP is not always desirable since excessive heating may be harmful to the surrounding tissues. Therefore, the challenge for shape-memory biomaterials is to be able to adjust their Tg close to body temperature, *i.e.* 37 °C, to avoid such issues. These materials could be easily inserted into the body through a small incision in a compressed, or elongated temporary shape, thereby minimizing surgery.

Our group recently showed that natural extruded thermoplastic starch presents an efficient shape-memory, without chemical grafting (Chaunier & Lourdin, 2009; Lourdin & Chaunier, 2009). Shape recovery of starch materials can be triggered by temperature as well as humidity. Water can diffuse into the polymer sample and acts as a plasticizer, leading to a Tg decrease to body temperature and even below (Chaunier & Lourdin, 2009; Leng et al., 2011; Vechambre et al., 2011).

The objective of this study was to demonstrate that shape-memory starch can be used for biomedical application. Unmodified potato starch was chosen due to its lack of residual components such as proteins or lipids that could have a harmful effect on its biocompatibility. Potato starch was extruded with water and glycerol as plasticizer. The mechanical properties and the structure of this SMP in both dry and in media-simulating physiological conditions (immersion in water at 37 °C) were assessed before and after sterilization. The shape-memory performances were evaluated in water at 37 °C and *in vivo* effects of the implantation of shape-memory extruded starch were determined after a subcutaneous implantation in a rat model.

2. Materials and methods

2.1. Raw materials

Potato starch was purchased from Roquette (Lestrem, France). The initial moisture content was approximately 13% of the wet basis weight (wb). Sodium bromide and 99% glycerol were purchased from Sigma–Aldrich Chemie GmbH (Steinheim, Germany). All other chemicals were obtained from Sigma–Aldrich Chemie GmbH (Steinheim, Germany) and used without further purification. Ultrapure milli-Q-water (18.3 MΩ cm^{-1}) (Millipore, Bedford, MA, USA) was used as a solvent.

2.2. Extrusion and sample equilibration

Prior to extrusion, water was added to adjust the starch moisture content to 27% wb. Glycerol content was adjusted to 20% (wb). Starch was mixed with water and glycerol in a laboratory kneading-machine.

Starch was extruded using a SCAMIA single-screw device (Rheoscam Type 20.11d, Crosne, France) with a die outlet diameter of 3 mm. The temperature profile was [100 °C; 110 °C; 110 °C] along the heating elements, from the entry of the extruder to its outlet (*i.e.* the die). The sample shape obtained was a dense, non-porous cylinder.

After flowing through the die, samples were stabilized in desiccators containing a saturated sodium bromide solution with a relative humidity (RH) of 59% at 20 °C for 15 days, in order to reach an equilibrated water content before subsequent analysis.

2.3. Sample sterilization

Extruded starch was submitted to sterilization by γ-ray ionization to evaluate the influence of ionization on their mechanical properties. γ-ray ionization was performed by Ionisos (Sablé-sur-Sarthe, France) at a minimal standardized dose of 25 kGy (ISO 11137) on samples stored in individual bags (Westfield Medical Limited, Midsomer Norton, UK). Samples were evaluated after being re-equilibrated at RH of 59%.

2.4. Sample characterization under ambient conditions

2.4.1. Mechanical properties

Tensile tests were carried out on starch cylinders (diameter = 3.4 mm; length = 50 mm) with a material testing machine (Instron Corporation, model 1122, Canton, MA, USA) equipped with a 100 N tensile load cell. The distance between grips was 20 mm and the crosshead speed was set at 5 mm min^{-1}. The elongation and the tensile stress at break (ε_r and σ_r, respectively) were evaluated at room temperature. Each measurement was performed at least five times.

2.4.2. Wide angle X-ray scattering (WAXS)

The crystalline structure was assessed by WAXS and diagrams were recorded in transmission mode using a Bruker D8 X-ray diffractometer (Madison, WI, USA) equipped with a two-dimensional GADDS detector. The X-ray radiation, Cu Kα1 (λ = 0.15405 nm), produced in a sealed tube at 40 kV and 40 mA was selected and parallelized using a Gobël mirror parallel optics system and collimated to produce a 500 μm beam diameter.

2.4.3. Differential scanning calorimetry (DSC)

The glass transition temperature was determined by DSC on an automated TA Q100 instrument (TA Instruments, New Castle, DE, USA). Experiments were carried out on an aliquot of approximately 10 mg of bulk sample placed in stainless steel airtight cells. Two successive scans were run at 3 °C min^{-1} between 0 and 160 °C, separated by a cooling stage. The glass transition temperature was determined on the second scan at the midpoint of the calorific capacity change on the thermogram.

2.4.4. Moisture content

Moisture content was determined for each sample after being stabilized over 15 days in a desiccator at RH = 59% at 20 °C by a thermo-gravimetric method. Briefly, samples were weighed and then heated in an oven at 130 °C for 24 h, then cooled down and reweighed. Moisture content was calculated based on the difference between these weights.

2.4.5. Molar mass determination

Samples (0.7 g) were first dissolved in 95% dimethylsulfoxide (DMSO) (20 mL) under magnetic stirring for 3 days at room temperature. Samples were then precipitated with ethanol (200 mL), rinsed with ethanol and dried with acetone, as previously described (Bello-Pérez, Roger, Baud, & Colonna, 1998). The precipitate was subsequently air-dried at room temperature under desiccant. As previously described (Rolland-Sabaté, Colonna, Mendez-Montealvo, & Planchot, 2007), the starch powder thus obtained was solubilized by microwave heating under pressure at 140 °C for 40 s. The starch solution was then filtered through a 5 μm Durapore® membrane (Waters, Bedford, MA, USA).

Molar masses were determined by asymmetrical flow field-flow fractionation coupled with multi-angle laser light scattering (AFFFF-MALLS) with a pure cellulose membrane at a cut-off point of 10,000 Da from Celgard LLB (Charlotte, NC, USA). Water was used as the mobile phase containing 0.2 g L^{-1} sodium azide, as previously described (Rolland-Sabaté et al., 2007), with a flow rate of 0.84 mL min^{-1} for channel flow in. The crossflow was set at 0.84 mL min^{-1} and the channel flow rate out was set at 0.2 mL min^{-1} for the sample introduction and relaxation/focusing period. The sample was injected at 0.2 mL min^{-1} for 300 s. After the injection pump was stopped, the sample was allowed to relax

and to focus for 60 s. For elution, the channel flow rate out was set at 0.84 mL min^{-1} and the crossflow was reduced from 0.4 to 0 mL min^{-1} for 400 s, after which it was maintained at 0 mL min^{-1} for 875 s. The concentrations were determined at each slice of the elugram using a differential refractometer RID-10A from Shimadzu (Kyoto, Japan).

To evaluate solubilization and elution recoveries, carbohydrate concentrations were determined by the sulfuric acid-orcinol colorimetric method (Tollier & Robin, 1979) both on the non-filtered and filtered solutions and by integration of the differential refractive index (DRI) signal.

Number and weight average molar masses, $\bar{M}_n$ and $\bar{M}_w$ were established as previously described (Rolland-Sabaté et al., 2007) using ASTRA® software from the Wyatt Technology Corporation (Santa Barbara, CA, USA) (version 5.3.4.20).

2.5. Sample evaluation in water at 37 °C

2.5.1. Water absorption

Water absorption of extruded starch was monitored as the sample was immersed in deionized water at 37 °C. Samples (diameter = 3.4 mm; length = 15 mm) were weighed before being immersed in deionized water. Samples were then periodically removed, gently dried on precision paper-wipes (Kimwipes®, Kimberly-Clark, VWR, France) and weighed before being re-dipped in water solution. Moisture content was then calculated based on the difference between the hydrated weight and the dry weight previously obtained.

2.5.2. Thermomechanical behavior

The dynamic mechanical analysis (DMA), carried out on a DMTA MKIV apparatus (Rheometric Scientific, Piscataway, NJ, USA), was used in the tensile mode with the frequency set at 1 Hz on starch cylinders (diameter = 3.4 mm; length = 15 mm). The deformation amplitude was 0.1%. The apparatus was turned upside down in order to measure the properties of the sample dipped in a deionized water bath thermostated at 37 °C. Data were collected by a computer program (RSI Orchestrator, Rheometric Scientific, Piscataway, NJ, USA), which calculated the dynamic properties E', E'' and $\tan\delta = E''/E'$, where E' is the storage or elastic modulus and E'' is the dissipative or viscous modulus.

2.6. Shape-memory properties

In order to make the extruded starch a shape-memory material, it is subjected to a thermomechanical history called programming steps. The permanent shape was the straight thread without any further modification after being extruded and cooled at 20 °C under a stable moisture level, RH = 59%. Then the temporary shape was given to the specimen after being heated above Tg. The sample was bent and cooled down while maintaining the mechanical bending before storage under Tg. Briefly, each straight starch cylinder (length = 50 mm) was immobilized on a bending device. Cylinders were bent to $\theta_0 = 180°$ after heating at Tg + 15 °C for 5 s. To fix the temporary shape, it was cooled down below Tg under constraint. Stress was then removed and the sample was stored at −20 °C before the recovery step.

To evaluate their shape recovery ability, the programmed shape-memory samples were immersed in water at 37 °C. Shape-memory performance of such bent samples was evaluated using a method previously described (Chaunier, Vechambre, & Lourdin, 2012; Lan, Liu, Lv, Wang, Leng, & Du, 2009; Leng et al., 2011). The recovery angle θ_n was closely monitored over time by a tri-CCD camera and VisionStage software (Alliance Vision, France). Images were then analyzed by Matlab® (MathWorks, France) to automatically calculate the recovered angle (θ_n) over time. Each experiment was performed at least five times for unsterilized and sterilized samples.

The recovery ratio (%) was calculated as:

$$R = \frac{\theta_0 - \theta_n}{\theta_0} \times 100$$

The recovery rate (° s^{-1}) was also evaluated by image-analysis.

2.7. In vivo sample implantation

2.7.1. Surgical procedure

The animal protocol was approved by Bichat University's Institutional Animal Care and Use Committee. Two independent sub-cutaneous pockets (1 cm) were made on either side of the abdominal wall midline in five anesthetized male Wistar rats (200–250 g, 8 weeks old, Janvier, CERJ, Laval, France) in order to avoid any contact or overlapping between samples during the post-operative period. Next, samples measuring 3.4 mm in diameter and 1 cm in length were inserted into these pockets. The skin was closed using Vicryl 4.0. At 8 days post-surgery, the rats were euthanized by an intraperitoneal injection of sodium pentobarbital (60 mg kg^{-1}). Implanted materials and the surrounding tissues were removed.

2.7.2. Histological studies

Implanted materials were dissected, and at least 0.5 cm of surrounding tissue was excised, gently rinsed in saline solution (9/1000) and fixed in 4% paraformaldehyde solutions, dehydrated and embedded in paraffin. Seven micron-thick sections were obtained per rat (Leitz Wetzlar microtome, France), stained with hematoxylin-eosin. Inflammatory reaction was also evaluated by macrophage immunostaining on tissue sections. Briefly, after paraffin removal and rehydration, sections were immersed in 3% hydrogen peroxide for 30 min and in 1% bovine serum albumin (BSA) for 40 min, then incubated with the primary antibodies: ED1 (mouse anti-rat CD68, 1:1000 in 1% BSA, Serotec, France) for 12 h at 4 °C, then incubated with an anti-mouse biotinylated secondary antibody 1 h (1:1000, in 1% Tris-BSA) at room temperature followed by HRP conjugated streptavidin (Dakocytomation, Denmark). Sections were exposed to diaminobenzidine substrate (DAB, Dakocytomation, Denmark) for 10 min and counterstained with hematoxylin. Sections were visualized under a microscope (Olympus, Tokyo, Japan) and photographed using Q Capture Pro software (Qimaging, Canada).

2.8. Statistical analysis

Statistical analyses were performed using Statgraphics Plus 5.1 software for Windows (StatPoint Technologies Inc., USA). *T*-tests were performed to evaluate the change between unsterilized and sterilized samples. $P < 0.05$ was considered as a significant difference between groups.

3. Results

3.1. Physical properties and structure of materials

3.1.1. Extrusion conditions and glass transition

The extrusion of potato starch previously hydrated at 27% wb and with 20% glycerol, led to translucent dense, non-porous cylinders 3.4 mm in diameter. With a screw speed of 20 rpm, the torque was approximately 6 N m and the pressure at the outlet of the extruder was close to 22 bar. The flow through the extruder was approximately 4.7 g min^{-1}. The specific mechanical energy was about 160 J g^{-1}.

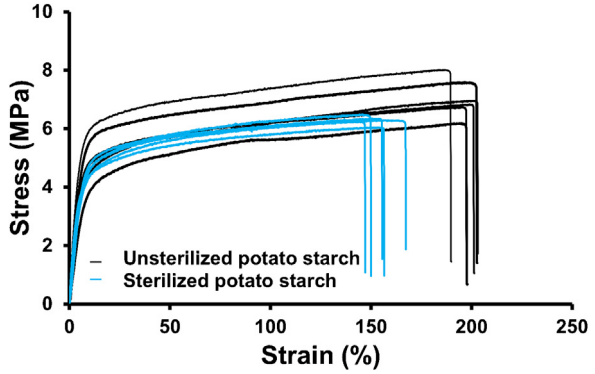

Fig. 1. Mechanical behavior of unsterilized and sterilized extruded starch samples conditioned at RH = 59% and 20 °C.

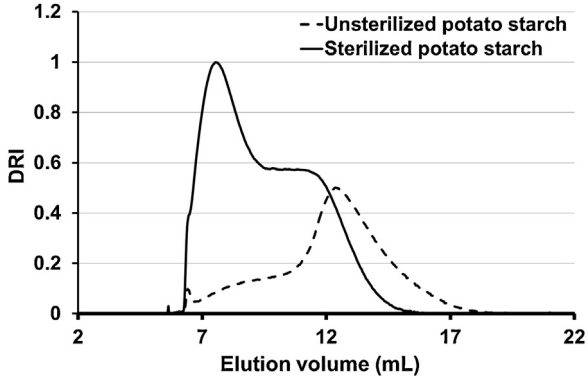

Fig. 2. Elugram of unsterilized and sterilized extruded starch samples obtained by AFFFF-MALLS (normalized differential refractive index, DRI).

Storage at equilibrated relative humidity (RH = 59%, 20 °C) led to a sample-moisture content of 13%, wb. The glass transition temperature was measured at 14 °C by DSC.

3.1.2. Effect of γ-rays on mechanical properties and molecular weight

After equilibration (RH = 59%, 20 °C), the elongation at break (ε_r) and the tensile stress at break (σ_r) were evaluated under ambient conditions on samples before and after γ-ray sterilization (Fig. 1). The mechanical properties given in Table 1 were found to be similar to those of previously published works (Vechambre, Chaunier, & Lourdin, 2010). Indeed, before sterilization, the tensile stress and elongation at break were 7.1 MPa and 206%, respectively (Table 1).

Stress–strain curves had the same profile before and after sterilization (Fig. 1), thus the γ-ray irradiation process did not seem to affect the mechanical behavior of the materials. Tensile stress and elongation at break decreased slightly after the ionizing treatment, from 7.1 ± 0.7 MPa to 6.4 ± 0.2 MPa and from 206 ± 17% to 155 ± 8%, respectively. Concerning the structure, the quasi-amorphous state of the samples, revealed by the WAXS diffractograms, was not modified by the γ-ray irradiation (data not shown).

The decrease of tensile stress and elongation at break may be explained by a depolymerization of amylose and amylopectin, which was confirmed by AFFFF-MALLS analysis. The elugram (Fig. 2) for unsterilized samples exhibited one main peak at 12.3 mL, representing amylopectin with a modal molar mass, or weight average molar mass, calculated using 10 slices at the apex of the amylopectin peak, $\bar{M}_w = 8.33 \times 10^7$ g mol^{-1}. The shoulder of this peak, between 7 and 10 mL of the elution volume represented the amylose component. On the elugram for sterilized samples, the amylopectin main peak was found at 11 mL with a molar mass of 6.81×10^6 g mol^{-1}. This shift to a smaller elution volume correlated to a smaller molar size revealing the degradation process due to the γ-ray treatment The main peak at 7.5 mL, with a modal molar mass $\bar{M}_w = 3.19 \times 10^5$ g mol^{-1}, would correspond to amylose and fragments of depolymerized amylopectin. The amylopectin depolymerization then induced a decrease of its molar mass and the production of dextrin chains of a size close to those of amylose, without the formation of small oligosaccharides, since the elution recovery was approximately 100% with the membrane cut-off of 10 kDa. Unfortunately, amylose degradation could not be evaluated by AFFFF-MALLS analysis because the elution method used was optimized for amylopectin fractionation.

Table 1
Effect of γ-rays irradiation on extruded starch samples conditioned at RH = 59% and 20 °C on mechanical properties and on shape recovery rate and recovery ratio.

	Unsterilized starch	Sterilized starch
Elongation at break (%)	206 ± 17	155 ± 8*
Tensile stress at break (MPa)	7.1 ± 0.7	6.4 ± 0.2*
Recovery rate (s^{-1})	6 ± 1	5 ± 1
Recovery ratio (%)	90 ± 4	93 ± 7

* $p < 0.05$, Student's test.

3.2. Thermomechanical properties and shape-memory performance determined in water at 37 °C

3.2.1. Thermomechanical properties and structure

The evolution of the mechanical modulus (E') of the material immersed in water at 37 °C was obtained by DMA analysis. The simultaneous water uptake was also measured. During the first 6 h, the storage modulus E' fell steeply from 1×10^9 Pa to about 2.4×10^6 Pa. Such a decrease of storage modulus was due to the increase of temperature from ambient temperature to 37 °C and simultaneously to the increase of water content from 12% to about 50%, wb (Fig. 3a). The moisture content then stabilized to

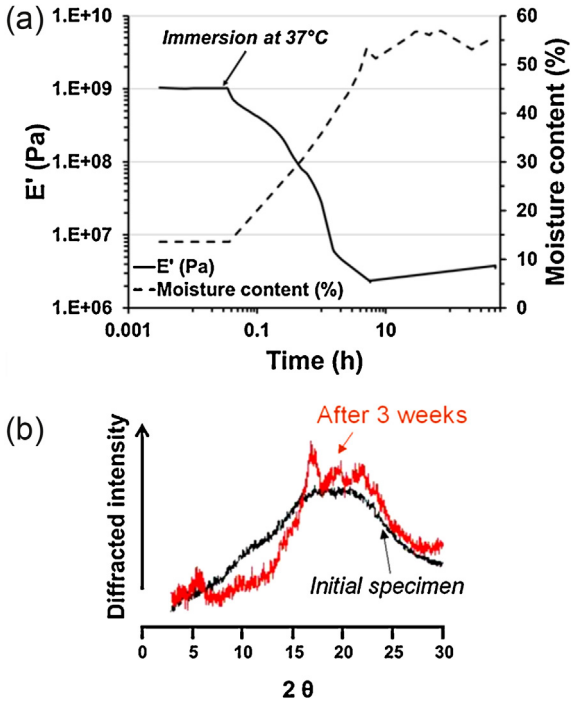

Fig. 3. Physical characterization upon immersion in water at 37 °C of extruded starch samples. (a) Mechanical properties determined by dynamic mechanical analysis (tensile mode). (b) WAXS diffractograms showing a crystallization process occurring during water immersion.

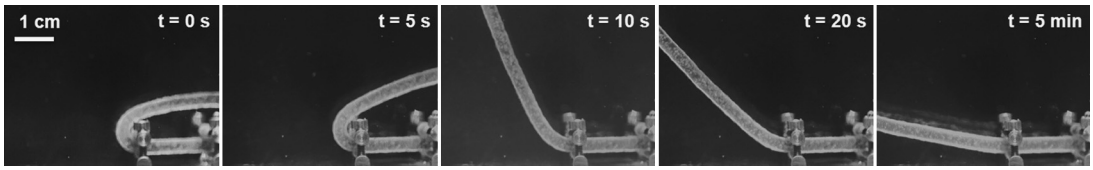

Fig. 4. Time-course of the extruded starch shape recovery followed by images acquisition. Self-deployment of a straight shape-memory extruded starch samples immersed in water at 37 °C.

approximately 55% after 24 h of immersion; the modulus remained almost stable and even slightly increased to 3.6×10^6 Pa, probably due to a slow crystallization that occured in starch. Indeed, the initial sample presented an almost amorphous structure as shown on the WAXS diffractogram (Fig. 3b). After being immersed for 3 weeks, the diffractogram of the sample revealed peaks at 5.6° and 17°. This corresponds to the crystalline hexagonal structure known as the B-type. The water uptake increased the mobility of amylose and amylopectin, leading to the emergence of a more organized semi-crystalline structure (Soest, Hulleman, de Wit, & Vliegenthart, 1996).

3.2.2. Shape recovery

Shape-memory properties were evaluated on straight extruded cylinders that were bent at 180° prior to the experiment and maintained as such at −20 °C without any constraint. The moisture content was not affected by this treatment. The sample was immersed in a water bath at 37 °C to relax the residual stresses and to allow the recovery of its initial shape, which took about 5 min (Fig. 4). The initial recovery rate and recovery ratio were evaluated by image analysis for both unsterilized and sterilized materials. Neither the shape recovery rate, about 5° s^{-1}, nor the shape recovery ratio, close to 90%, was affected by the sterilization process, as shown in Table 1. Moreover, 80% of the shape recovery occurred in less than 20 s.

3.3. Sample in vivo implantations

In order to determine the tissue reaction to starch material, an *in vivo* study was performed in a rat model. Samples were easily implanted and the thread was not broken by the suture knot. The samples (Fig. 5a) were left for 8 days to study the short-term host–tissue reaction. After explantation, no macroscopic signs of inflammation or infection were seen. After 8 days, the samples were still observed (yellow dotted line) but degraded (Fig. 5c, blue arrows) within a matrix containing fibroblasts and inflammatory cells, mainly macrophages (Fig. 5b, arrows), surrounded by a thin fibrotic capsule (Fig. 5c, green arrow).

4. Discussion

Shape-memory properties of extruded starch materials have been largely demonstrated in previous work (Vechambre et al., 2011; Vechambre, Buleon, Chaunier, Jamme, & Lourdin, 2010; Vechambre et al., 2010b). In order to envisage the domain of biomedical applications, with a great potential for shape-memory polymers (Yakacki et al., 2007), the shape recovery in body conditions remained to be demonstrated for starch materials. In particular it was necessary to investigate the duration of shape recovery which is a crucial aspect for these applications. In this study, the properties were measured on a 3.4 mm diameter cylinder of extruded starch containing 20% glycerol. The complete shape-recovery time after immersion in water at 37 °C was obtained in 5 min. Moreover, 80% of the shape recovery occurred in less than 20 s. Such shape-recovery time obtained in thermal physiological conditions is coherent for biomedical devices and is comparable with other usual biomaterials. For example, the recovery time at 37 °C for a poly-L-lactic acid (PLLA) stent 0.17 mm in thickness is about 20 min (Tamai et al., 2000). Yakacki and coworkers have shown that a tube with a wall thickness of 0.3 mm made from tert-butyl acrylate, di(ethylene glycol) dimethacrylate and poly(ethylene glycol) dimethacrylate co-polymer will recover in 10 s to 10 min, depending on the crosslinking ratio (Yakacki et al., 2007). Other SMP such as a co-polymer from caprolactone and microbial polymer 0.21 mm in thickness will recover in 25 s (Xue, Dai, & Li, 2010). Beyond these data which depend on the geometry of the device, what is most interesting is the possibility to optimize the recovery time according to the application. This can be obtained with starch materials thanks to the very wide domain of Tg, heavily dependent on plasticizer and water contents. Fig. 6 represents the state diagram showing glass transition with water content for potato starch containing 0 and 20% glycerol from data previously published (Lourdin, Coignard, Bizot, & Colonna, 1997). The crossing

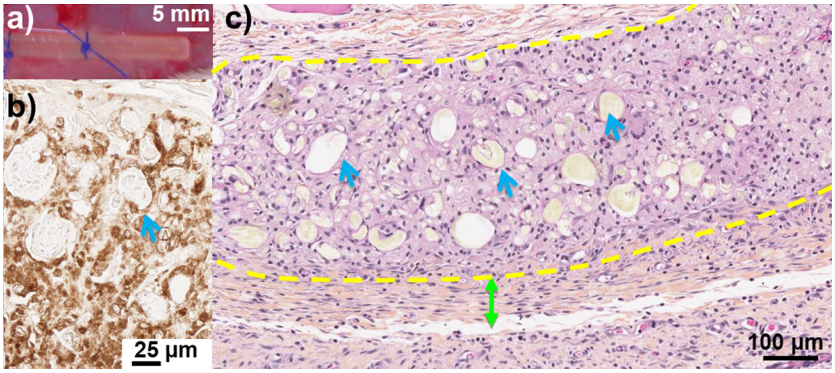

Fig. 5. Implantation and histological studies. A 1 cm length extruded starch sample was implanted in subcutaneous pocket in rat abdominal wall (a). (c) After 8 days post-surgery, samples were still visible (yellow dotted line). A thin fibrotic cap surrounding samples were observed (green arrow). At higher magnification (b), starch particles (blue arrows) were surrounded by many cells in a non-organized extracellular matrix. At day 8, macrophages were detected by CD68 immunostaining (brown). (For interpretation of the references to color in this figure legend, the reader is referred to the web version of the article.)

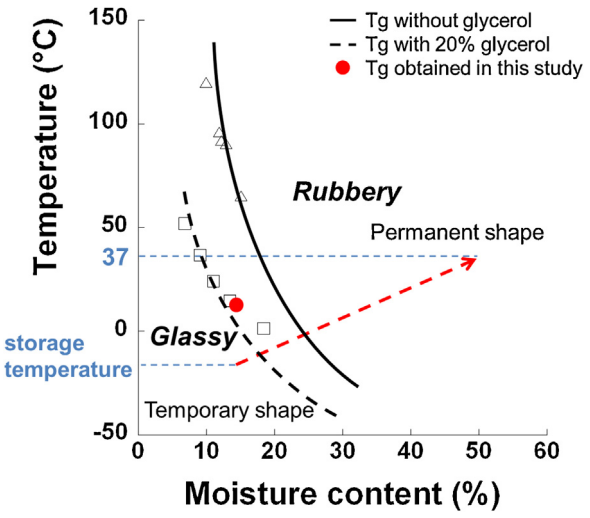

Fig. 6. State diagram representing Tg evolution with water content, from data published previously (Lourdin, Coignard, Bizot, & Colonna, 1997). Red arrow indicates the starting and the destination point of temperature/moisture change during sample immersion. Red point indicates experimental data obtained in this study. (For interpretation of the references to color in this figure legend, the reader is referred to the web version of the article.)

of Tg which trigger shape recovery is symbolized by the red arrow indicating the starting and the destination point of temperature/moisture change during sample immersion. In this study, the glassy/rubbery transition is the consequence of the sample heating from storage temperature (−20 °C in the present case) to body temperature (37 °C) and also by the water diffusion into the sample (from 13% to about 50%), acting as a plasticizer for starch-based materials. It appears clearly that these mechanisms and consequently the rate and extent of shape recovery are controlled by the position of the Tg/water content curve. This curve can be switched depending on glycerol content (Lourdin et al., 1997). Thus, a wide range of recovery times can be controlled from a few seconds to minutes by adjusting the amount of glycerol in the composition.

Because of the hydrophilic nature of starch, a modification of the mechanical properties of samples immersed in water is inevitable. Indeed, the elastic modulus (E') of samples decreased during the first hours of immersion, corresponding to a water uptake of nearly 50% wb. After 10 hours, due to the crystallization, the elastic modulus E' is stabilized at around 3 MPa and remained constant for the next 40 days of immersion. The material remains rubbery, deformable and easy to handle.

The impact of the sterilization process on the physical properties of biomaterials is a key issue for the future use of this material as a medical device. On extruded starch, a depolymerization of amylopectin by the ionizing treatment was revealed. For amylose it is less clear, but a fragmentation of linear chains can be suspected. Despite this molecular degradation, the tensile stress and elongation at break remain at a correct level. Regarding the shape-memory properties, there are not altered by the sterilization process carried out on the permanent shape. Globally it can be considered that the sterilization treatment by γ-radiation at the standard minimal dose required for biomedical application does not strongly affect physical properties of starch materials. To compare to other biodegradable medical devices such as PLLA, a degradation after sterilization at 25 kGy was observed and led to a decrease of stiffness since crystallinity increased (Kantoglu & Guven, 2002; Suljovrujic et al., 2007). This probably resulted from an alteration of the polymer structure due both to crosslinking and chain-scission (Milicevic, Milivojevic, & Suljovrujic, 2012).

Starch-based scaffolds have demonstrated great potential applications in the fields of tissue engineering (Gomes, Godinho, Tchalamov, Cunha, & Reis, 2002; Neves et al., 2005; Sobral, Caridade, Sousa, Mano, & Reis, 2011) or as biomaterials (Frost et al., 2011; Rodrigues & Emeje, 2012; Torres, Troncoso, Grande, & Diaz, 2011). Generally they are used in association with other compounds such as chitosan (Martins et al., 2012), polycaprolactone (Santos et al., 2010), gelatin (Zhang et al., 2013). In this study we studied *in vivo* responses of 100% starch-based samples. Our results showed a good extracellular matrix organization surrounding the residual starch samples and a limited inflammatory reaction, mainly due to the presence of the macrophages, thus promoting the starch-based sample resorption. This observation is a part of a normal wound-healing response to implanted biomaterials (Anderson, Rodriguez, & Chang, 2008) and these results were similar to those obtained with starch-hydrid samples such as chitosan/starch (Martins et al., 2012) or starch/polycaprolactone (Santos et al., 2010) scaffolds where moderate inflammation are observed after 8 days' implantation. While the resorption is fast for these 100% starch- based scaffolds, and may represent a limitation for some medical applications which require slow resorption time, this could be improved by using different extruded botanical sources, to extend the *in vivo* lifespan of those materials. On the other hand, this property could be used in some clinical applications which require a quick time-resorption, due to a high local amylase activity, without inducing inflammatory responses such as salivary-stenting.

5. Conclusion

Starch was extruded to create a new biomaterial with shape-memory properties. We demonstrated that shape recovery can be triggered in media-simulating body conditions. Due to the ability for crystallization, starch materials show interesting and stable mechanical properties during a long period in water at 37 °C. Moreover, starch possesses good biocompatibility and biodegradability in a rat model. Programmed samples recover their initial shape in a very short time, which allows applications in outpatient surgery, thus minimizing the need for anesthesia and reducing hospitalization time. The thermoplastic properties of starch are conducive to the design of a very complex temporary and permanent 3D shape. All these characteristics indicate that extruded starch is a good candidate for the development of medical devices with shape-memory properties.

Acknowledgments

The authors would like to thank C. Véchambre, A. Buléon, R. Désirest, M. de Carvalho, A-L. Réguerre, A. Rolland-Sabaté and B. Pontoire (INRA, Nantes) and L. Louedec and F. Medjahed (INSERM, Paris) for their technical help and helpful discussions. This work has been funded by the French National Research Agency (ANR Emergence IRMAS-EMMA-007).

References

Anderson, J. M., Rodriguez, A., & Chang, D. T. (2008). Foreign body reaction to biomaterials. *Seminars in Immunology*, *20*(2), 86–100.

Arockianathan, P. M., Sekar, S., Kumaran, B., & Sastry, T. P. (2012). Preparation, characterization and evaluation of biocomposite films containing chitosan and sago starch impregnated with silver nanoparticles. *International Journal of Biological Macromolecules*, *50*(4), 939–946.

Bello-Pérez, L. A., Roger, P., Baud, B., & Colonna, P. (1998). Macromolecular features of starches determined by aqueous high-performance size exclusion chromatography. *Journal of Cereal Science*, *27*(3), 267–278.

Buléon, A., Colonna, P., Planchot, V., & Ball, S. (1998). Starch granules: Structure and biosynthesis. *International Journal of Biological Macromolecules*, *23*(2), 85–112.

Chaunier, L., & Lourdin, D. (2009). The shape memory of starch. *Starch – Stärke*, *61*(2), 116–118.

Chaunier, L., Vechambre, C., & Lourdin, D. (2012). Starch-based foods presenting shape memory capabilities. *Food Research International*, *47*(2), 194–196.
Frost, K., Barthes, J., Kaminski, D., Lascaris, E., Niere, J., & Shanks, R. (2011). Thermoplastic starch silica–polyvinyl alcohol composites by reactive extrusion. *Carbohydrate Polymers*, *84*(1), 343–350.
Ghosh, S., Gutierrez, V., Fernandez, C., Rodriguez-Perez, M. A., Viana, J. C., Reis, R. L., et al. (2008). Dynamic mechanical behavior of starch-based scaffolds in dry and physiologically simulated conditions: Effect of porosity and pore size. *Acta Biomaterialia*, *4*(4), 950–959.
Gomes, M. E., Godinho, J. S., Tchalamov, D., Cunha, A. M., & Reis, R. L. (2002). Alternative tissue engineering scaffolds based on starch: Processing methodologies, morphology, degradation and mechanical properties. *Materials Science and Engineering: C*, *20*(1–2), 19–26.
Gomes, M. E., Ribeiro, A. S., Malafaya, P. B., Reis, R. L., & Cunha, A. M. (2001). A new approach based on injection moulding to produce biodegradable starch-based polymeric scaffolds: Morphology, mechanical and degradation behaviour. *Biomaterials*, *22*(9), 883–889.
Guo, B., Chen, Y., Lei, Y., Zhang, L., Zhou, W. Y., Rabie, A. B. M., et al. (2011). Biobased poly(propylene sebacate) as shape memory polymer with tunable switching temperature for potential biomedical applications. *Biomacromolecules*, *12*(4), 1312–1321.
Hayakawa, I., Linko, Y. Y., & Linko, P. (1996). Novel mechanical treatments of biomaterials. *Food Science and Technology*, *29*(5–6), 395–403.
Kantoglu, O., & Guven, O. (2002). Radiation induced crystallinity damage in poly(L-lactic acid). *Nuclear Instruments and Methods in Physics Research Section B: Beam Interactions with Materials and Atoms*, *197*(34), 259–264.
Lan, X., Liu, Y., Lv, H., Wang, X., Leng, J., & Du, S. (2009). Fiber reinforced shape-memory polymer composite and its application in a deployable hinge. *Smart Materials and Structures*, *18*(2), 024002.
Lendlein, A., Behl, M., Hiebl, B., & Wischke, C. (2010). Shape-memory polymers as a technology platform for biomedical applications. *Expert Review of Medical Devices*, *7*(3), 357–379.
Lendlein, A., & Kelch, S. (2002). Shape-memory polymers. *Angewandte Chemie (International Edition in English)*, *41*(12), 2035–2057.
Leng, J., Lan, X., Liu, Y., & Du, S. (2011). Shape-memory polymers and their composites: Stimulus methods and applications. *Progress in Materials Science*, *56*(7), 1077–1135.
Liu, C., Qin, H., & Mather, P. T. (2007). Review of progress in shape-memory polymers. *Journal of Materials Chemistry*, *17*(16), 1543–1558.
Lopez, O. V., Lecot, C. J., Zaritzky, N. E., & Garcia, M. A. (2011). Biodegradable packages development from starch based heat sealable films. *Journal of Food Engineering*, *105*(2), 254–263.
Lourdin, D., & Chaunier, L. (2009). Shape memory composition comprising starch. Patent WO/2009/130215, France.
Lourdin, D., Coignard, L., Bizot, H., & Colonna, P. (1997). Influence of equilibrium relative humidity and plasticizer concentration on the water content and glass transition of starch materials. *Polymer*, *38*(21), 5401–5406.
Martins, A. M., Kretlow, J. D., Costa-Pinto, A. R., Malafaya, P. B., Fernandes, E. M., Neves, N. M., et al. (2012). Gradual pore formation in natural origin scaffolds throughout subcutaneous implantation. *Journal of Biomedical Materials Research Part A*, *100A*(3), 599–612.
Milicevic, D., Milivojevic, D., & Suljovrujic, E. (2012). The influence of the initial preparation and crystallinity on the free radical evolution in gamma irradiated PLLA. *Radiation Physics and Chemistry*, *81*(9), 1361–1365.
Neves, N. M., Kouyumdzhiev, A., & Reis, R. L. (2005). The morphology, mechanical properties and ageing behavior of porous injection molded starch-based blends for tissue engineering scaffolding. *Materials Science and Engineering: C*, *25*(2), 195–200.
Oliveira, J., Crawford, A., Mundy, J., Moreira, A., Gomes, M., Hatton, P., et al. (2007). A cartilage tissue engineering approach combining starch-polycaprolactone fibre mesh scaffolds with bovine articular chondrocytes. *Journal of Materials Science: Materials in Medicine*, *18*(2), 295–302.
Rodrigues, A., & Emeje, M. (2012). Recent applications of starch derivatives in nanodrug delivery. *Carbohydrate Polymers*, *87*(2), 987–994.
Rolland-Sabaté, A., Colonna, P., Mendez-Montealvo, M. G., & Planchot, V. (2007). Branching features of amylopectins and glycogen determined by asymmetrical flow field flow fractionation coupled with multiangle laser light scattering. *Biomacromolecules*, *8*(8), 2520–2532.
Santos, T. C., Marques, A. P., Höring, B., Martins, A. R., Tuzlakoglu, K., Castro, A. G., et al. (2010). In vivo short-term and long-term host reaction to starch-based scaffolds. *Acta Biomaterialia*, *6*(11), 4314–4326.
Sobral, J. M., Caridade, S. G., Sousa, R. A., Mano, J. O. F., & Reis, R. L. (2011). Three-dimensional plotted scaffolds with controlled pore size gradients: Effect of scaffold geometry on mechanical performance and cell seeding efficiency. *Acta Biomaterialia*, *7*(3), 1009–1018.
Suljovrujic, E., Ignjatovic, N., Uskokovic, D., Mitric, M., Mitrovic, M., & Tomic, S. (2007). Radiation-induced degradation of hydroxyapatite/poly L-lactide composite biomaterial. *Radiation Physics and Chemistry*, *76*(4), 722–728.
Tamai, H., Igaki, K., Kyo, E., Kosuga, K., Kawashima, A., Matsui, S., et al. (2000). Initial and 6-month results of biodegradable poly-L-lactic acid coronary stents in humans. *Circulation*, *102*(4), 399–404.
Tollier, M.-T., & Robin, J.-P. (1979). Adaption de la méthode à l'orcinol-sulfurique au dosage automatiques des glucides neutres totaux: Conditions d'application aux extraits d'origine végétale. *Annales de Technologie Agricole*, *28*(1), 1–15.
Torres, F. G., Troncoso, O. P., Grande, C. G., & Diaz, D. A. (2011). Biocompatibilty of starch-based films from starch of Andean crops for biomedical applications. *Materials Science and Engineering: C*, *31*(8), 1737–1740.
van Soest, J. J. G., Hulleman, S. H. D., de Wit, D., & Vliegenthart, J. F. G. (1996). Changes in the mechanical properties of thermoplastic potato starch in relation with changes in B-type crystallinity. *Carbohydrate Polymers*, *29*(3), 225–232.
Vechambre, C., Buleon, A., Chaunier, L., Gauthier, C., & Lourdin, D. (2011). Understanding the mechanisms involved in shape memory starch: Macromolecular orientation, stress recovery and molecular mobility. *Macromolecules*, *44*(23), 9384–9389.
Vechambre, C., Buleon, A., Chaunier, L., Jamme, F., & Lourdin, D. (2010). Macromolecular orientation in glassy starch materials that exhibit shape memory behavior. *Macromolecules*, *43*(23), 9854–9858.
Vechambre, C., Chaunier, L., & Lourdin, D. (2010). Novel shape-memory materials based on potato starch. *Macromolecular Materials and Engineering*, *295*(2), 115–122.
Xue, L., Dai, S., & Li, Z. (2010). Biodegradable shape-memory block co-polymers for fast self-expandable stents. *Biomaterials*, *31*(32), 8132–8140.
Yakacki, C. M., Shandas, R., Lanning, C., Rech, B., Eckstein, A., & Gall, K. (2007). Unconstrained recovery characterization of shape-memory polymer networks for cardiovascular applications. *Biomaterials*, *28*(14), 2255–2263.
Zhang, N., Liu, H., Yu, L., Liu, X., Zhang, L., Chen, L., et al. (2013). Developing gelatin-starch blends for use as capsule materials. *Carbohydrate Polymers*, *92*(1), 455–461.